Adaptive fast sliding neural control for robot manipulator

Barış ÖZYER[*]
Computer Engineering Department, Faculty of Engineering, Atatürk University, Erzurum, Turkey

Abstract: Robotic manipulators are open to external disturbances and actuation failures during performing a task such as trajectory tracking. In this paper, we present a modifed controller consisting of a global fast sliding surface combined with an adaptive neural network which is called adaptive fast sliding neural control (AFSNC) for a robotic manipulator to precise stable trajectory tracking performance under the external disturbances. The adaptive term is employed to reduce uncertainties due to unmodeled dynamics. Tracking error asymptotically converges to zero according to the Lyapunov stability theorem. Numerical examples have been carried on a planar two-links manipulator to verify the control approach efficiency. The experimental results show that the proposed control approach performs satisfactory trajectory tracking and tracks the desired trajectory in less time with reduced chattering effect compared to the other methods.

Key words: Sliding mode control, adaptive control, neural network control, asmyptotic stability, robot manipulator

1. Introduction

The integrated robotic platforms such as arm and end-effector have been available in the industry to perform different simple tasks such as pick and place, screwing, drilling, welding and etc. for the last decades. These robots basically need to follow the desired trajectory in a high constraint environment in order to successfully achieve all these tasks. However, in real applications, even if having a motion controller, it is not easy due to uncertainty parameters from the unknown environment and nonlinear dynamical behavior of robot manipulators. During the last decades, many researchers have been interested in designing control algorithms for achieving robust trajectory such as variable structure control method, intelligent control, PID control, torque control, adaptive control and etc. [1–6].

Because of having a basic mathematical model, PID control algorithm has been mostly employed in various applications among the industrial robotic manipulators, where parameters of the dynamic model are accurately known [7]. The stability of the system depends on operating speed which should be slow enough to converge the parameters and setting the initial condition of robot motions. It has been arguing that PID control algorithm cannot handle nonlinear systems having uncertainty parameters in high speed applications. On the other hand, it is required that robotic manipulators ultimately overcome this uncertainty for tracking robust trajectory [8]. Computed torque control (CTC) based on feed back linearization has applicable performance in high speed applications [9]. However, CTC is not useful in practical application because this method needs an exact dynamic model of robots and is not stable when subjected to uncertainty. Computed torque control based adaptive control algorithms are used to handle uncertainty regarding the unknown parameters due to payload

[*]Correspondence: baris.ozyer@atauni.edu.tr

3154

disturbances and friction coefficients [10]. Although it is verified that the adaptive controller is asymptotically stable in the Lyapunov sense in the case that manipulator is subjected to bounded external disturbances, it cannot handle unmodelled dynamic parameters. The well known variable structure control method which is sliding mode control (SMC), which is a popular variable structure control method, is combined with the adaptive controller to achieve asymptotic convergence infinite time where dynamic parameters of the manipulator are not exactly known [11]. The SMC is based on switching control law that includes two phases. The sliding surface is firstly necessary to be determined where the state variable should be designed to follow the desired trajectory in joint coordinates for any bounded disturbances. The second one is adjusting to determine switching gain that should be larger than bounded unknown disturbance and dynamic parameters [12]. SMC is highly robust against system uncertainties that are unknown in the real world. During the sliding phase, the control signal switches fastly to handle the disturbance effect. However, the error occurs on the path tracked by the manipulator during the reaching phase. Terminal sliding mode (TSM) control is designed to estimate uncertainties that improve the transient response such as faster convergence to equilibrium and better robustness when comparing with SMC [13, 14]. However, the singularity problem still exists to be observed in control inputs. In [15], a global nonsingular terminal sliding mode (NTSM) control is designed to cope with singularity problem of nonlinear dynamical systems. In [16], the two phases described as reaching and sliding are adjusted by applying TSM to achieve global finite-time stability. In TSM and conventional SMC, both the stability and tracking performance is not robust under the disturbances caused by uncertainties of the parameters of the dynamic system during the reaching phase. Integral sliding mode (ISM) control approach is designed to obtain robust trajectory tracking performance [17]. Besides, fast terminal sliding mode (FTSM) control is proposed that the controller satisfies fast transient convergence under single-input single-output transition mode [18].

As mentioned above, various types of sliding mode controller have been proposed to satisfy robust tracking. However, the well-known chattering phenomena that leads to accuracy reduction and inefficient control performance is still a big challenge. The main reasons for the chattering in the nonlinear control system are high-frequency switching leading to the control of the signal oscillation, discontinuity of input signal and damaging in the physical system. When the nonlinear system is controlled by a sliding approach under the uncertainty, high-frequency control signal oscillations can be adjusted that lead to robust control. However, the chattering effect cannot be fully eliminated. To perform high precision tracking performance under the chattering effect, adaptive control techniques combined with sliding mode control have been developed [19–21]. Combining these two techniques is effective enough to eliminate unknown disturbances and dynamic parameters but not exactly handle the chattering effect. In [22], global adaptive sliding mode control approach is proposed. According to the study, the chattering problem is considerably diminished and steady state error approximates very small values under the uncertainty and nonlinearity of the dynamical system. Since unknown dynamic parameters and external disturbances are not completely modeled in the real application, chattering effect cannot be fully eliminated and the chattering free sliding mode control model is not obtained. It is necessary to apply smooth a control signal to the system. Among other studies in the literature, various ISM control and high order sliding mode (HOSM) algorithms are presented to perform a robust position control strategy for the robotic manipulator to reduce the chattering effect [23, 24]. Increasing the degree of the designed sliding mode manifold with integrators, it is possible to obtain smooth control signal. There is another approach proposed in [25], upper and lower boundaries of the switching surface are used for diminishing the chattering effect.

In the last past decade, artificial intelligence and machine learning approaches have been adapted in a nonlinear controller to overestimate the switching gains that reduce the chattering effect [26–28]. Neural network

and fuzzy-based algorithms are widely investigated in order to approximate the nonlinear dynamic parameters for different types of manipulator such as rigid and flexible manipulator [27, 29]. The neural network algorithm is capable of approximating any nonlinear continuous function which is used in the manipulator controllers. On the other hand, computational time increases significantly as increasing the number of the sample in the neural network in the nonlinear system to estimate the upper bound uncertainties. In [30], adaptive radial basis function (RBF) neural network control is proposed to learn the unknown upper bound uncertainties without the prior knowledge of the system. The integrated fuzzy neural network is applied to a nonlinear dynamical system which has fast learning capability to approximate unknown parameters [31]. In most control system, the outputs, such as position or velocity, or two of them, are measured directly. On the other hand, external disturbance parameter cannot be measured directly. The fundamental issue here is that it is necessary to estimate unmeasured states from measurable variables in order to achieve exponential stability. Several disturbance observer design methods based on SMC have been proposed to eliminate unmeasured external disturbances and chattering phenomenon [32–35].

In this study, we design an adaptive fast sliding neural control (AFSNC) for robot manipulator to handle the external bounded uncertainties which is revised from the model [36]. Motivation of the paper is to achieve robust tracking performance on reference trajectories as fast as possible. It is modified that the global fast sliding surface presented in [18] and [37] is combined with an adaptive neural network that satisfies asymptotically stable for any initial condition. Radial basis function is used to estimate nonlinear function in the designed neural network [38]. It is proved that the tracking errors asymptotically converge to zero. Experimental results show that our proposed approach has good performance for trajectory tracking. It is worth to point out that the designed controller achieves to compensate external disturbances and reduces chattering effect [39].In order to demonstrate the effectiveness of the AFSNC, it is compared with the conventional SMC, sliding mode control based on radial basis function neural network (NNSMC) [38] and neural network-based sliding mode adaptive control (NNSMAC) [39].

The rest of this paper is organized as follows: Problem formulation including the dynamic model of the manipulator, proposed controller design approaches, brief theories, and their proofs are given in Section 2. Numerical experimental results on two-link manipulator simulation are illustrated and discussed in Section 3. Section 4 concludes this paper and gives the future direction of our studies.

2. Problem definition
Let us consider the n-link manipulator that the general dynamic model is described by following equation [36]

$$\mathbf{D(q)\ddot{q}} + \mathbf{C(q,\dot{q})\dot{q}} + \mathbf{F(\dot{q})} + \mathbf{g} + \lambda_{\mathbf{d}} = \lambda, \tag{1}$$

where $\mathbf{q}$ is position, $\dot{\mathbf{q}}$ is velocity and $\ddot{\mathbf{q}}$ is acceleration of the joints $\in R^n$. $\mathbf{D(q)} \in R^{nxn}$, $\mathbf{C(q,\dot{q})} \in R^{nxn}$, $\lambda_{\mathbf{d}}, \mathbf{g} \in R^{nx1}$ and $\lambda \in R^{nx1}$ respectively refers to the positive definite symmetric inertia matrix, the coriolis matrix, the bounded disturbance, the gravity torque and the input torque vector. $\mathbf{F(\dot{q})}$ is the friction term described by the following equation:

$$F(\dot{q}) = F_v\dot{q} + F_d, \tag{2}$$

where F_v is the viscous friction coefficient and F_d is the Coulomb friction torque.

Property 1 $D(q)$ is assumed to satisfy upper and lower boundaries represented as

$$\mu_1 < \| \mathbf{D}(\mathbf{q}) \| < \mu_2, \tag{3}$$

where μ_1 and μ_2 are positive constant and $\| \, . \, \|$ denotes the induced matrix norm of $D(q)$ matrix.

Property 2 Coriolis $C(q, \dot{q})$ matrix in $\dot{q}$ variable satisfies following equation

$$x^T (\dot{\mathbf{D}}(\mathbf{q}) - 2\mathbf{C}(\mathbf{q}, \dot{\mathbf{q}}))x = 0, \tag{4}$$

where $(\dot{\mathbf{D}} - 2\mathbf{C}(\mathbf{q}, \dot{\mathbf{q}}))$ is skew symmetric matrix and it is bounded as $\| \mathbf{C} \| \le v_b$, where v_b is positive constant.

Property 3 The gravitational torque $\| g \| \le \rho$ is bounded where $0 < \rho < \infty$

Remark 1: The disturbance torque is considered as norm-bounded described as

$$\| \lambda_d \| \le \lambda_0 < \infty. \tag{5}$$

It is noticed that the disturbance parameter λ can be either measurable or not.

2.1. Controller design

In this section, as shown in Figure 1, we present a modified controller consisting of global fast sliding mode control combined with an adaptive and neural network for n-link robot manipulator. The main strategy of designing the controller is that the joint position of robot manipulator q follows to the joint reference position q_d in a stable manner where the tracking error converges to zero. The dynamic equation of the manipulator is assumed to be known and joints position and velocity are measurable.
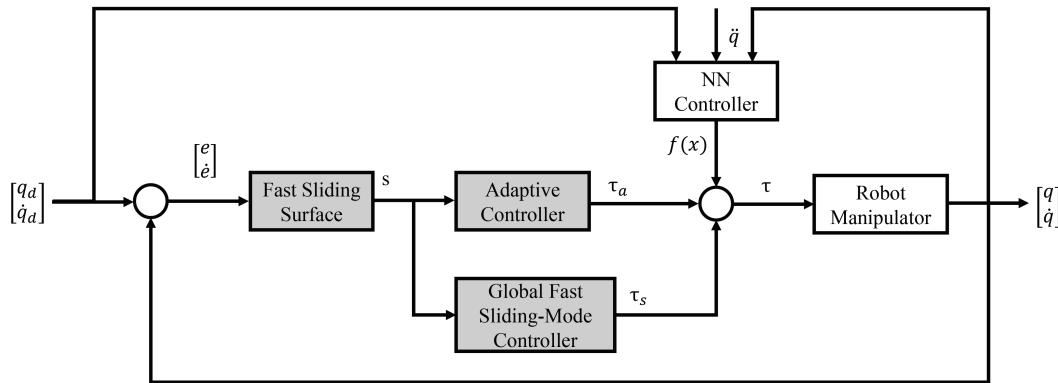

Figure 1. The proposed adaptive fast sliding neural control model (AFSNC). The system model is revised from the model in [36, 39]. Modified control parameters is represented in gray box.

2.1.1. Fast sliding surface design

Designing sliding surface, which is one of the contribution modified from [39], is most important part of achieving robust control in nonlinear system. The tracking error is described as $\mathbf{e} = \mathbf{q_d} - \mathbf{q}$ where q_d is the desired joint reference position. The fast sliding surface [37] s is defined as

$$s = \dot{\mathbf{e}} + \varphi_1 \mathbf{e} + \varphi_2 \mathbf{diag}(|\mathbf{e_1}|, ..., |\mathbf{e_n}|)^r sgn(\mathbf{e}) = 0, \tag{6}$$

where $\varphi_1 = diag(\varphi_{11}, \varphi_{12}, ..., \varphi_{1n}) \in R^{nxn}$ and $\varphi_2 = diag(\varphi_{21}, \varphi_{22}, ..., \varphi_{2n}) \in R^{nxn}$ are positive definite matrices, $r = \kappa_1/\kappa_2$, error vector is $\mathbf{e} = [e_1, ..., e_n]^T \in R^n$ with $0 \leq |e_i| \leq a$ where upper bound $a > 0$, κ_1 and κ_2 are positive odd integers and κ_2 is greater than κ_1. According to the theory [37], when the system state moves away from the equilibrium point, the linear term $\varphi_1 \mathbf{e}$ is dominated. When the system state approaches to equilibrium point, the power term $\varphi_2 \mathbf{e}^{\kappa_1/\kappa_2}$ term is dominated that improves the system convergence. Therefore, the sliding surface converges to zero for any given initial condition in finite definite time t_c at the equilibrium point defined as [37]

$$t_c = \frac{\kappa_1}{\|\varphi_1\|(\kappa_1 - \kappa_2)} ln \frac{\|\varphi_1\| q_0(0)^{(r-1)} + \|\varphi_2\|}{\|\varphi_2\|}, \tag{7}$$

where $\|.\|$ is the induced matrix norm. For any given initial condition such that $q_0(0) \neq 0$, the system converges to zero in finite time t_c. The time derivative of the sliding surface is calculated as

$$\dot{s} = \ddot{\mathbf{e}} + \varphi_1 \dot{\mathbf{e}} + \varphi_2 \mathbf{r} diag(|\mathbf{e_1}|^{\mathbf{r-1}}, ..., |\mathbf{e_n}|^{\mathbf{r-1}}) \dot{\mathbf{e}}. \tag{8}$$

Let us consider second order nonlinear system that $\dot{x_1} = x_2$ and $\dot{x_2} = z(x) + c(x)u + \lambda_d$ where $z(x)$ and $c(x)$ is the smooth function, λ_d is the bounded uncertainties and $x_1 = e$ [38]. The fast sliding mode controller is described as follows:

$$u(t) = -\frac{1}{c(x)}(z(x) + \dot{\mathbf{e}} + \varphi_1 \mathbf{e} + \varphi_2 diag(|\mathbf{e_1}|^{\mathbf{r}}, ..., |\mathbf{e_n}|^{\mathbf{r}}) sgn(\mathbf{e}) + \psi s + \gamma s^r). \tag{9}$$

The equation (8) is rewritten as

$$\dot{s} = z(x) + c(x)u + \lambda_d + \varphi_1 \dot{\mathbf{e}} + \varphi_2 \mathbf{r} diag(|\mathbf{e_1}|^{\mathbf{r-1}}, ..., |\mathbf{e_n}|^{\mathbf{r-1}}) \dot{\mathbf{e}}. \tag{10}$$

Then, we obtain,

$$\dot{s} = -\psi s - \gamma s^r. \tag{11}$$

Consider Lyapunov function candidate selected as below

$$V = \frac{1}{2} s^T s. \tag{12}$$

The differentiation V with respect to time is

$$\begin{aligned}
\dot{V} &= s^T \dot{s} \\
&= -s^T \varphi_1 s - s^T \varphi_2 diag(|s_1|^{r-1}, ..., |s_n|^{r-1}) sgn(s) \\
&= -s^T \varphi_1 s - sgn(s^T) \varphi_2 diag(|s_1|^{r-1}, ..., |s_n|^{r-1}) sgn(s) \\
&\leq -\nu_{min}\{\varphi_1\} \|s\|^2 - \nu_{min}\{\varphi_2\} sgn(s^T) diag(|s_1|^{r-1}, ..., |s_n|^{r-1}) sgn(s) \\
&\leq -\nu_{min}\{\varphi_1\} \|s\|^2 - \nu_{min}\{\varphi_2\} \|s\|_{l_1} \\
&\leq -\psi \|s\|^2 - \gamma \|s\|_{l_1}
\end{aligned} \tag{13}$$

where $\psi > 0$, $1 < \gamma < 2$ and $\|.\|_{l_1}$ is the induced l_1 norm of s.

2.1.2. Adaptive fast sliding mode neuro controller design

From Equations (1) and (8), the arm dynamic can be described on the fast sliding surface as

$$\mathbf{D(q)\dot{s}} = \mathbf{C_s} - \lambda_\mathbf{d} + \lambda + \mathbf{f(x)}, \tag{14}$$

where the nonlinear function $\mathbf{f(x)}$ due to uncertainties is obtained as

$$\mathbf{f(x)} = \mathbf{D(q)}[\ddot{\mathbf{q}}_\mathbf{d} + \varphi_1\dot{\mathbf{e}} + \varphi_2\frac{d(\mathbf{e}^{\kappa_1/\kappa_2})}{dt}] + \mathbf{C}[\dot{\mathbf{q}}_\mathbf{d} + \varphi_1\mathbf{e} + \varphi_2\mathbf{e}^{\kappa_1/\kappa_2}] + \mathbf{F(\dot{q})} + \mathbf{g}, \tag{15}$$

where the vector x is the states of the system described as $\mathbf{x} = [q^T, \dot{q}^T, q_d^T, \dot{q_d}^T, \ddot{q_d}^T]^T \in R^{5n}$. The estimated nonlinear function of $\mathbf{f(\tilde{x})} = R^l \leftrightarrow R^m$ is given as

$$\tilde{f}(x) = \tilde{W}^T\phi(x), \tag{16}$$

where $\tilde{\mathbf{W}} = [w_1, ..., w_b] \in R^{mxb}$ are the estimated RBF NN weight matrices and $\phi(\mathbf{x}) = [\phi_1(x), ..., \phi_b(x)]$ is selected as Gaussian Radial Basis Function defined as

$$\phi_\mathbf{i}(\mathbf{x}) = \exp^{\frac{1}{2\sigma_i^2}(\mathbf{x}-\mu_\mathbf{i})^T(\mathbf{x}-\mu_\mathbf{i})} \ i = 1, ..., b \tag{17}$$

where $\mu_\mathbf{i} = [\mu_{i1}, ..., \mu_{il}]$ is the mean vector and $\sigma_\mathbf{i}$ is the variance of the Gaussian function. The dynamic equation can be rewritten as

$$\mathbf{D(q)\dot{s}} = -\mathbf{C_s} + \tilde{\mathbf{W}}\phi(\mathbf{x}) + \hat{\mathbf{W}}\phi(\mathbf{x}) + \lambda_\mathbf{d} + \lambda, \tag{18}$$

where $\hat{\mathbf{W}} = \mathbf{W}^* - \tilde{\mathbf{W}}$ and $\mathbf{W}^*$ represents the ideal weight matrices [39].

Theorem-1 Consider the system shown in Figure 1, the input torque of the manipulator λ is designed as

$$\lambda = \lambda_\mathbf{s} + \lambda_\mathbf{a} + \lambda_\mathbf{nn}, \tag{19}$$

where $\lambda_\mathbf{s}$, $\lambda_\mathbf{a}$, $\lambda_\mathbf{nn}$ denotes sliding mode control, adaptive control and neural control inputs of the manipulator, respectively.

The sliding controller input [36, 38] is defined as

$$\lambda_\mathbf{s} = -k_1s - k_2sgn(s), \tag{20}$$

where k_1 and k_2 is greater than 0 and for any initial state the trajectory will reach on sliding surface $s = 0$ in finite time.

Remark 2: In fact, determining the effective control input is difficult due to unknowns in actual system parameters and unmodeled dynamics uncertainties. We have added an adaptive term in the proposed system to reduce the effect of uncertainties.

The adaptive control input $\lambda_\mathbf{a}$ is defined as [39]

$$\lambda_\mathbf{a} = \xi s, \tag{21}$$

where $\xi > 0$ is the variable of adaptive law.

Remark 3: Chattering due to discontinuous *sgn* function of sliding mode controller leads to instability of the system. RBF Neural networks with suitable adaptive law is used to reduce the chattering problem.

The RBF neural network controller λ_{nn} is described in (16) as $\hat{f}(x)$ with unknown parameters [39] defined as

$$f(\hat{x}) = -\dot{\hat{W}}^T \phi(\mathbf{x}) + \epsilon, \tag{22}$$

where $\hat{\mathbf{W}}$ is the weight estimated error matrices and ϵ is the variable of approximation error is bounded that satisfies following equations

$$\|\epsilon\| \leq \|f(x) + \mathbf{W^T}\phi(\mathbf{x})\|. \tag{23}$$

It is assumed that weights tunning can be described as

$$\dot{\hat{\mathbf{W}}} = \mathbf{Q}\phi(\mathbf{x})s, \tag{24}$$

where $\mathbf{Q}$ is a positive definite matrix. The tracking errors $\mathbf{e}$ and $\dot{\mathbf{e}}$ approaches to zero on the sliding surface, that is the nonlinear system is asymptotically stable.

Proof : The candidate Lyapunov function [36, 38, 39] is described as

$$L = \frac{1}{2}s^T\mathbf{D}(\mathbf{q})s + \frac{1}{2}tr\{\tilde{\mathbf{W}}\mathbf{Q^{-1}}\tilde{\mathbf{W}}\} + \tilde{\xi}s, \tag{25}$$

where $\tilde{\xi}^T = \xi - \xi_d$ and $tr(.)$ is the trace of a matrix. The differentiation of L with respect to time is calculated by

$$\begin{aligned}
\dot{L} &= s^T\mathbf{D}(\mathbf{q})\dot{s} + \frac{1}{2}s^T\dot{\mathbf{D}(\mathbf{q})}s + tr\{\tilde{\mathbf{W}}\mathbf{Q^{-1}}\dot{\tilde{\mathbf{W}}}\} + \dot{\tilde{\xi}}s \\
&= -k_1 s^T s - k_2 s^T sgn(s) + s^T\mathbf{Q}\phi(\mathbf{x})s - s^T\xi s + s^T(\dot{\epsilon} + \dot{\lambda}_d) \\
&\quad + \frac{1}{2}s^T(\mathbf{M}(\dot{\mathbf{q}}) - \mathbf{2C})s + tr\{\tilde{\mathbf{W}}\mathbf{Q^{-1}}\dot{\tilde{\mathbf{W}}}\} + \dot{\tilde{\xi}}s
\end{aligned} \tag{26}$$

where $\dot{\tilde{\xi}} = \frac{1}{\|s\|^2 + \rho}$ with ρ is bounded constant that satisfies $\int_0^\infty \rho dt < \infty$ and approximation error [39]. It assumed that approximation error and disturbance is bounded, then derivation terms goes to zero. Since $\mathbf{D}(\mathbf{q})$ is the skew symmetric positive definite matrix and from Equations (11), (13) and (24), the following equation is obtained:

$$\dot{L} \leq -k_{1min}\|s\|^2 - k_2|s| + \varphi_0\|s\|^2 \tag{27}$$

,

where $\varphi_0 = 1/\xi$ is the positive constant. By integrating the differential Equation (27) from $t = 0$ to T as below:

$$|L(T) - T(0)| \leq \int |-k_{1min}\|s\|^2 - k_2|s| + \varphi_0\|s\|^2|dt. \tag{28}$$

For $t \in [0, T]$, $L(T) \geq 0$ and there exists

$$\lim_{t \to \infty} \sup_t \int_0^T \|s\|^2 dt \leq \lim_{t \to \infty} (\frac{1}{k_1} + \frac{1}{k_2} + \varphi_0)L(0)$$
$$= 0$$
(29)

then every solution for candidate Lyapunov function L, it implies that the tracking error $\mathbf{e}$ and $\dot{\mathbf{e}}$ converges to zero as $s \to 0$ based on Equations (6) and (22), and the system is asymptotically stable.

3. Simulation results

The proposed AFSNC is tested by applying numerical simulations on the two link planar manipulator. The numerical parameters of the simulation are assumed as the mass of the joints $m_1 = m_2 = 1kg$, the length of the links $l_1 = l_2 = 1m$, the gravity term $g = 9.8m/s^2$. The initial values of state vector is chosen as $x(0) = [0.9, 0.4, 0.5, 3.0, 0.5, 0]^T$. The fast sliding surface parameters are assumed as $\kappa_1 = 2.5$, $\kappa_2 = 1.5$, $\varphi_1 = diag\{20, 20\}$, $\varphi_2 = diag\{3000, 3000\}$. The bound uncertainty parameters such as external disturbances and unknown dynamic parameter of the system in (5) is assumed to be $0 < \lambda_{d_i} < 1$ where $i = 1, 2$. The desired trajectory is given as $q_{d1}(t) = 0.1cos(0.5t)$ and $q_{d2}(t) = 0.1sin(0.5t)$. The initial NN weights W are set to zero. The number of hidden layer is determined by heuristically evaluating from 5 to 15 and then is set to 12. The input vector of the NN is defined as Equation (15). The control parameters are set as follows: Q=diag$\{20,20\}$ and $C = diag\{15, 15\}$ [38]. The Gaussian radial basis function is set to zero mean and $\sigma_1 = \sigma_2 = \sqrt{2}$ variance. Since RBF neural network is expressed as linearly parameterized form, candidate Lyapunov function given in Equation (25) is selected and then updated laws for unknown parameters is estimated. The NN weights are updated online by Equation (24) in order to satisfy the trajectory tracking. The adaptation law ξ is selected as 10 in our proposed method. The sampling period is chosen 5 ms.

The numerical simulation results are shown in Figures 2–6. The actual and corresponding to the desired position of joint trajectories are depicted in Figure 2 where the conventional SMC, NNSMC, NNSMAC, and proposed AFSNC controller applied. It is indicated in the figures that conventional SMC has a slower response and more chattering than the other methods. NNSMC and NNNSMAC have better robust performance than conventional SMC in the presence of unknown parameters due to NN structure. The proposed controller successfully tracks the reference trajectory within less time and the minimum-maximum overshoot is obtained for both two joints when compared with all other algorithms to the sliding surface design. Figure 3 shows the actual and desired angular velocity of joint trajectories. From the spectrum of velocity, it is verified that the proposed method converge to desired velocity trajectory faster than the other methods within minimum fluctuations.

Figure 4 depicts the control inputs λ_1, λ_2 generated by SMC, NNSMC, NNSMAC, and proposed AFSNC controller. As it is expected that the biggest chattering is observed in SMC from the initial moment of movement to the reaching phase. The control input pattern of NNSMC and NNSMAC is almost the same and reduces the chattering when compared with SMC. As seen from the figure that the proposed AFSNC method has a significant effect on reducing chattering among all control algorithms. This is particularly because that the neural network with adaptation law is applied to approximate unknown parameters that adapt the switching gain. The control input of the proposed method reaches to target values less than 2 s that shows the best performance among the other methods. Adaptation law ξ is important to chattering reduction that affects trajectory performance. If ξ is selected very small value, we observed a huge amount of chattering.
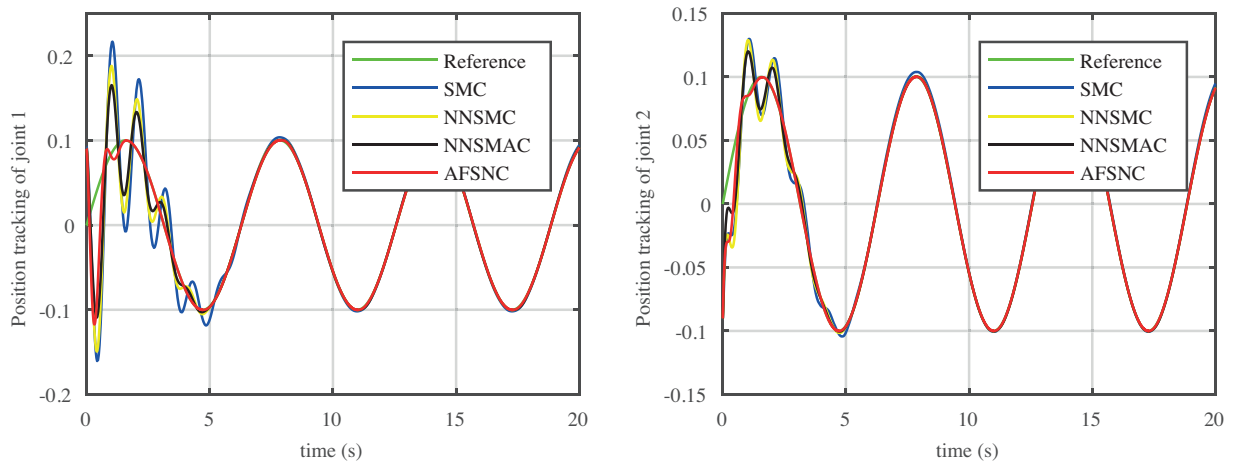
Figure 2. The actual position tracking performance of joint 1 and joint 2. The reference positions q_{d_i} for each joints $i \in \{1, 2\}$ are compared with the results of proposed AFSNC method and the other SMC, NNSMC [38] and NNSMAC [39] methods. (a) joint 1 (b) joint 2.
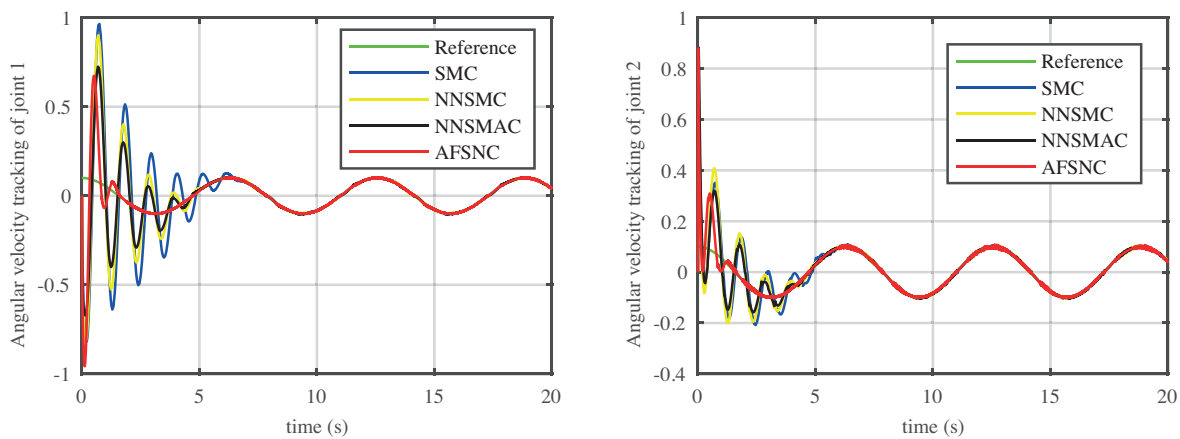

Figure 3. The angular velocity tracking performance of joint 1 and joint 2. The reference angular velocities $\dot{q}_{d_i}$ for each joints $i \in \{1, 2\}$ are compared with the results of proposed AFSNC method and the other SMC, NNSMC [38] and NNSMAC [39] methods. (a) joint 1 (b) joint 2.

The tracking error is caused by uncertainties, bounded disturbance and chattering effects. Figure 5 shows the convergence of tracking error for each two links after applying conventional SMC, NNSMC, NNSMAC, and proposed AFSNC controller. It is indicated that tracking errors asymptotically converge to zero for all methods in case the initial tracking error value is same. In our proposed method, tracking error converges at 1.6 s which is faster than the other methods. The reason is neural network weights converge to finite value much faster in our result and adaptive law guarantees asymptotic stability of error. To compare the results more accurately, root mean squared (RMS) values for both two joints are given in Table. As it is expected, trajectory performance as shown in Figure 1 is improved that leads to successfully follow the desired q_d position trajectory.

As shown in Figure 6, compared with NNSMC and NNSMAC, the estimated RBF neural network function defined as f(x̂) converges to f(x) less than 2 s in proposed method. While the estimated weights $\hat{W}$ converge to its true value, the tracking error converges to zero as shown in Figure 5. NN structure provides self learning
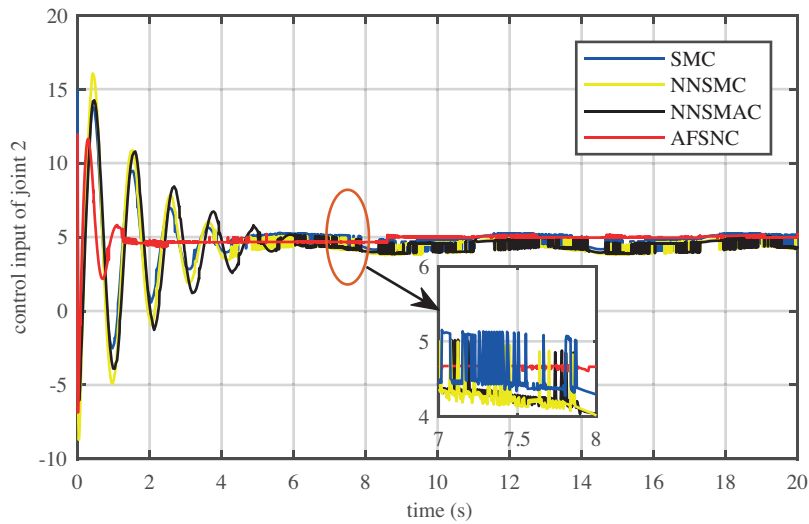
(a) Control input torque λ_1 for joint 1
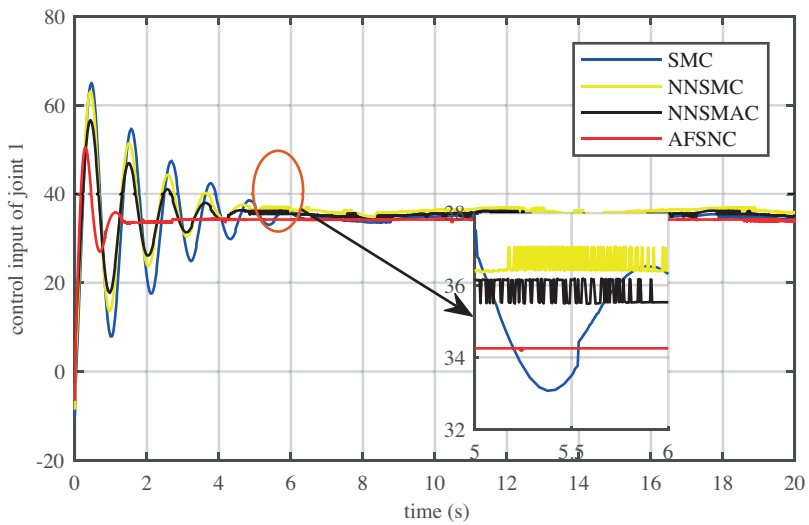
(b) Control input torque λ_1 for joint 2

Figure 4. The comparison control input performance of proposed AFSNC method with SMC, NNSMC [38] and NNSMAC [39] methods. (a) joint 1 (b) joint 2.

Table . RMS values of the tracking error.

Control methods	Joint 1	Joint 2
SMC	0.0185	0.0082
NNSMC	0.0150	0.0078
NNSMAC	0.0128	0.0066
AFSNC(proposed)	0.0087	0.0045

ability to the controller. The approximation function depends on the initial state variables and gaussian function parameters that are selected as experimentally. The main issue here is that neural network weights are updated
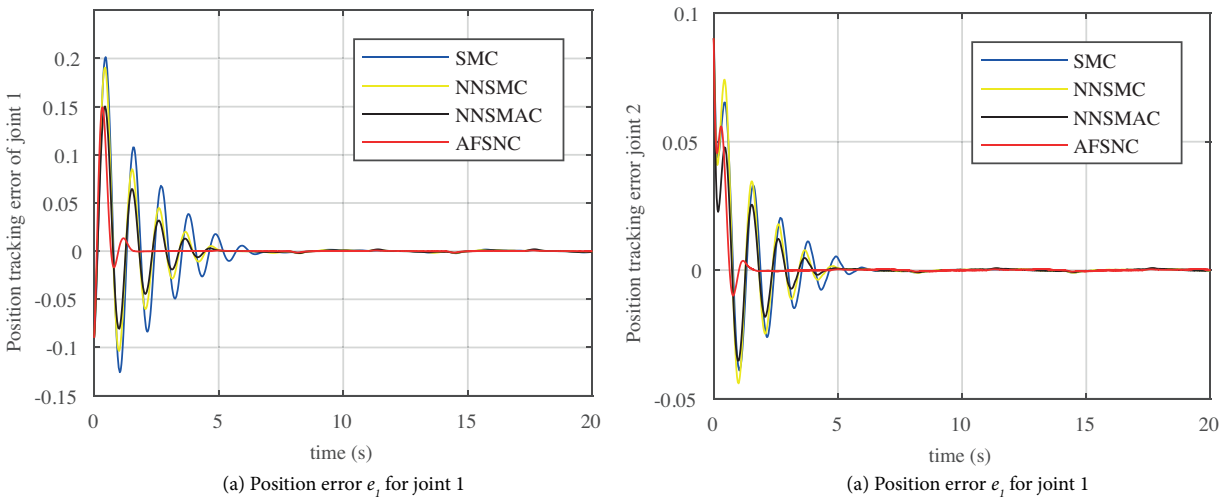
(a) Position error e_i for joint 1

(a) Position error e_i for joint 1

Figure 5. The comparison position tracking error ($e = q - q_d$) performance under uncertainties, bounded disturbance and chattering effects between proposed AFSNC method with SMC, NNSMC [38] and NNSMAC [39] methods. (a) joint 1 (b) joint 2.

by considering the tracking error. Compared to other methods, our proposed RBF neural network with selected adaption law has better learning performance and efficient tracking performance. We can conclude that the numerical simulation results verify the theoretical approximation.
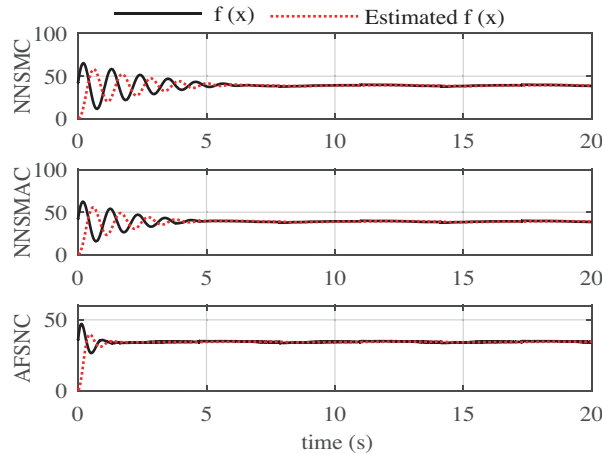

Figure 6. The nonlinear function f(x) and the estimated radial basis neural network nonlinear function $\hat{f}(x)$ under NNSMC, NNSMAC and proposed AFSNC methods. The proposed AFSNC estimated function converges to f(x) function less than 2 s.

4. Conclusion

In this paper, a new AFSNC controller is proposed for achieving robust trajectory tracking. The proposed approach basically contains a fast sliding surface design that is combined with adaptive neural network algo-rithms. RBF neural network with a new adaptation law is used for reducing the chattering effect. In addition, unmodeled uncertainties are eliminated. The stability condition of the sliding surface proved that sliding surface

converges to zero for any initial condition. Thus, it is proved by the Lyapunov theorem that the nonlinear system is asymptotically stable. We conducted several numerical simulation experiments using reference trajectories to validate the performance of the AFSNC controller. To verify and test the effectiveness of our approaches, AFSNC is compared with SMC, NNSMC, and NNSMAC methods. It is clearly observed that the proposed AF-SNC converges to the desired trajectory in less time than the other methods. The robust tracking performance under disturbances with bounded error is obtained and the chattering problem is significantly reduced.

The load on a gripper is another issue that effects the robustness of trajectory tracking. As a future work, physical interaction and force feedback from the environment is considered based on trajectory tracking. In addition, the performance of proposed approach is going to be tested on real robots.

References

[1] Kelly R. A tuning procedure for stable pid control of robot manipulators. Robotica 2015; 13 (2): 141-148.

[2] Parra VV, Arimoto S, Liu YH, Hirzinger G, Akella P. Dynamic sliding pid control for tracking of robot manipulators: theory and experiments. IEEE Transactions on Robotics and Automation 2003; 19 (6): 967-976 .

[3] He W, Dong Y, Sun C. Adaptive neural impedance control of a robotic manipulator with input saturation. IEEE Transactions on Systems, Man and Cybernetics Systems 2016; 46 (3): 334-344.

[4] Achili B, Daachi B, Amirat Y, Cherif A. A robust adaptive control of a parallel robot. International Journal of Control 2010; 83 (10): 2107-2119. doi: 10.1080/00207179.2010.505965

[5] Wang F, Chao Z, Huang LB, Li HY, Zhang CQ. Trajectory tracking control of robot manipulator based on RBF neural network and fuzzy sliding mode. Cluster Computing 2017; 22 (3): 5799-5809.

[6] Zhao D, Li S, Gao F. A new terminal sliding mode control for robotic manipulators. International Journal of Control 2009; 82 (10): 1804-1813.

[7] Cervantes I, Alvarez-Ramirez J. On the pid tracking control of robot manipulators. Systems & Control Letters 2001; 42 (1): 37-46.

[8] Song Z, Yi J, Zhao D, Li X. A computed torque controller for uncertain robotic manipulator systems: Fuzzy approach. Fuzzy Sets and Systems 2005; 15 (2): 208-226.

[9] Yang Z, Wu J, Mei J. Motor-mechanism dynamic model based neural network optimized computed torque control of a high speed parallel manipulator. Mechatronics 2007; 17 (7): 381-390.

[10] Mrad FT, Ahmad S. Adaptive control of flexible joint robots using position and velocity feedback. International Journal of Control 1992; 55 (5): 1255-1277.

[11] Zeinali M, Notash L. Adaptive sliding mode control with uncertainty estimator for robot manipulators. Mechanism and Machine Theory 2010; 45 (1): 80-90.

[12] Kali Y, Saad M, Benjelloun K, Benbrahim M. Sliding mode with time delay control for robot manipulators. In: Derbel N, Ghommam J, Zhu Q (editors). Applications of Sliding Mode Control. Studies in Systems, Decision and Control. Singapore: Springer, 2017, pp. 135-156.

[13] Asl RM, Hagh YS, Palm R. Robust control by adaptive non-singular terminal sliding mode. Engineering Applications of Artificial Intelligence 2017; 59: 205-217.

[14] Neila MBR, Tarak D. Adaptive terminal sliding mode control for rigid robotic manipulators. International Journal of Automation and Computing 2011; 8 (2): 215-220.

[15] Feng Y, Yu X, Man Z. Non-singular terminal sliding mode control of rigid manipulators. Automatica 2002; 38 (12): 2159-2167.

[16] Yu S, Yu X, Shirinzadeh B, Man Z. Continuous finite-time control for robotic manipulators with terminal sliding mode. Automatica 2005; 41 (11): 1957-1964.

[17] Utkin V, Shi J. Integral sliding mode in systems operating under uncertainty conditions. In: Proceedings of 35th IEEE Conference on Decision and Control; Kobe, Japan; 1996. pp. 4591-4596.

[18] Yu X, Zhihong M. Fast terminal sliding-mode control design for nonlinear dynamical systems. IEEE Transactions on Circuits and Systems I: Fundamental Theory and Applications 2002; 49 (2): 261-264.

[19] Baek J, Jin M, Han S. A new adaptive sliding-mode control scheme for application to robot manipulators. IEEE Transactions on Industrial Electronics 2016; 63 (6): 3628-3637.

[20] Hutama I, Kuo CH. Adaptive sliding mode control of a 6-dof rled robot manipulator with uncertain parameters and external disturbances. International Journal of Automation and Smart Technology 2016; 6 (1): 13-24.

[21] Wang H. Adaptive control of robot manipulators with uncertain kinematics and dynamics. IEEE Transactions on Automatic Control 2017; 62 (2): 948-954.

[22] Mobayen S. An adaptive fast terminal sliding mode control combined with global sliding mode scheme for tracking control of uncertain nonlinear third-order systems. Nonlinear Dynamics 2015; 82: 599-610. doi: 10.1007/s11071-015-2180-4

[23] Salah L, Plestan F, Glumineau A. Higher order sliding mode control based on integral sliding mode. Automatica 2007; 43 (2): 531-537.

[24] Zhang L, Liu L, Wang Z, Xia Y. Continuous finite-time control for uncertain robot manipulators with integral sliding mode. IET Control Theory and Applications 2018; 12 (11): 1621-1627.

[25] Kachroo P, Tomizuka M, Chattering reduction and error convergence in the sliding-mode control of a class of nonlinear systems. IEEE Transactions on Automatic Control 1996; 41 (7): 1063-1068.

[26] Wang L, Chai T, Zhai L. Neural-network-based terminal sliding-mode control of robotic manipulators including actuator dynamics. IEEE Transactions on Industrial Electronics 2009; 56 (9): 3296-3304.

[27] Lin FJ, Shen PH. Robust fuzzy neural network sliding-mode control for two-axis motion control system. IEEE Transactions on Industrial Electronics 2006; 53 (4): 1209-1225.

[28] Akyüz IH, Bingül Z, Kizir S. Cascade fuzzy logic control of a single-link flexible-joint manipulator. Turkish Journal of Electrical Engineering & Computer Sciences 2012; 20(5): 713-726.

[29] Sun G, Gao H, He W, Yu Y. Fuzzy neural network control of a flexible robotic manipulator using assumed mode method. IEEE Transactions on Neural Networks and Learning Systems 2018; 29 (11): 5214-5227.

[30] Fei J, Ding H. Adaptive sliding mode control of dynamic system using RBF neural network. Nonlinear Dynamics 2012; 70 (2): 1563-1573.

[31] Wai RJ, Muthusamy R. Fuzzy-neural-network inherited sliding-mode control for robot manipulator including actuator dynamics. IEEE Transactions on Neural Networks and Learning Systems 2012; 24 (2): 274-287.

[32] Shtessel Y, Edwards C, Fridman L, Levant A. Conventional sliding mode observers. In: William SL (editor). Sliding Mode Control and Observation. Birkhäuser, NY, USA: Springer, 2014, pp.105-141.

[33] Spurgeon SK. Sliding mode observers: a survey. International Journal of Systems Science 2008; 39 (8): 751-764.

[34] Chen WH, Yang J, Guo L, Li S. Disturbance-observer-based control and related methods—an overview. IEEE Transactions on Industrial Electronics 2016; 63 (2): 1083-1095.

[35] Chairez I, Poznyak A, Poznyak T. New sliding-mode learning law for dynamic neural network observer. IEEE Transactions on Circuits and Systems II: Express Briefs 2006; 53 (12): 1338-1342.

[36] Lewis FL, Lewis DM, Abdallah CT. Neural Network Control of Robots. In: Munro N, Lewis LL (editors). Robot Manipulator Control: Theory and Practice. 2nd ed. New York, NY, USA: CRC Press, 2004, pp.431-462.

[37] Liang X, Li S, Fei J. Adaptive fuzzy global fast terminal sliding mode control for microgyroscope system. IEEE Access 2016; 4: 9681-9688.

[38] Liu J, Wang X. RBF Network Adaptive Sliding Mode Control for Manipulator. In: Liu J, Wang X (editors). Advanced Sliding Mode Control for Mechanical Systems. Berlin, Germany: Springer, 2012, pp. 300-313.

[39] Sun T, Pei H, Pan Y, Zhou H, Zhang C. Neural network-based sliding mode adaptive control for robot manipulators. Neurocomputing 2011; 74 (14-15): 2377-2384.

Appendix

Dynamic model equations of two link manipulator

The general form of the dynamic model of the two link robotic manipulator given in Equation (4) [36] is described as

$$D(q)\ddot{q} + C(q,\dot{q})\dot{q} + g = \lambda,$$

where the positive definite inertia matrix $D(q) \in R^{2x2}$ and the coriolis matrix $C(q,\dot{q}) \in R^{2x2}$ is defined as

$$D(q) = \begin{bmatrix} D_{11} & D_{12} \\ D_{21} & D_{22} \end{bmatrix} \quad C(q,\dot{q}) = \begin{bmatrix} C_{11} & C_{12} \\ C_{21} & C_{22} \end{bmatrix}$$

$$D_{11} = (m_1 + m_2)l_1^2 + m_2 l_2^2 + 2m_2 l_1 l_2 cos(\theta_2)$$

$$D_{22} = m_2 l_2^2$$

$$D_{12} = D_{21} = m_2 l_2^2 + m_2 l_1 l_2 cos(\theta_2)$$

$$C_{11} = -\dot{\theta}_2 m_2 l_1 l_2 sin(\theta_2) \quad C_{12} = -(\dot{\theta}_1 + \dot{\theta}_2)m_2 l_1 l_2 sin(\theta_2)$$

$$C_{21} = \dot{\theta}_1 m_2 l_1 l_2 sin(\theta_2) \quad C_{22} = 0$$

where θ_1 and θ_2 are joint angles, $\dot{\theta}_1$ and $\dot{\theta}_2$ joint velocities, m_1 and m_2 are masses, l_1 and l_2 are the lengths of the link 1 and 2. The gravity matrix $g \in R^{2x1}$ is defined as

$$G_{11} = (m_1 + m_2)gl_1 cos(\theta_1) + m_2 gl_2 cos(\theta_1 + \theta_2)$$

$$, G_{21} = m_2 gl_2 cos(\theta_1 + \theta_2).$$

Preliminaries of fast sliding mode control

The sliding surface is designed based on the following formulations. The signum function $sgn(x)$ of the real variable $x \in (-\infty, \infty)$ is defined as

$$sgn(x) = \begin{cases} 1 & , x > 0 \\ 0 & , x = 0 \\ -1 & , x < 0 \end{cases}$$

Based on this definition, we can write a real vector $\mathbf{x} \in R^n$ over the real number field $R \in (-\infty, \infty)$ as follows:

$$\mathbf{x} = [|x_1|sgn(x_1), |x_2|sgn(x_2), ..., |x_n|sgn(x_n)]^T$$

$$= diag(|x_1|, |x_2|, ..., |x_n|)sgn(\mathbf{x}),$$

where $sgn(\mathbf{x}) \in R^n$ is the component wise signum vector function. The component wise power real vector function $\mathbf{x}^r$ of the real vector $\mathbf{x}$ with any positive real number $r \in (0, \infty)$ is defined as

1

$$\mathbf{x}^r = [|x_1|^r sgn(x_1), |x_2|^r sgn(x_2), ..., |x_n|^r sign(x_n)]^T$$
$$= diag(|x_1|, |x_2|, ..., |x_n|)^r sgn(\mathbf{x})$$
$$= diag(|x_1|^r, |x_2|^r, ..., |x_n|^r) sgn(\mathbf{x}) \in R^n.$$

So, we have n-dimensional real vector with components any positive power function $\mathbf{x}_i^r = |x_i|^r sgn(x_i)$ for $i = \{1, 2, ..., n\}$ to be integrable bounded real function passing through state space origin.

The derivative of the $sgn(x)^r$ is defined as follows:

$$\frac{d}{dt}(sgn(x)^r) = r|x|^{r-1}\dot{x}.$$